Dynamical Evolution of Planetesimals in the Outer Solar System

I. The Jupiter/Saturn Zone

Kevin R. Grazier

Jet Propulsion Laboratory, California Institute of Technology, Pasadena, California, 91109

William I. Newman

Departments of Earth and Space Sciences, Physics and Astronomy, and Mathematics, University of California, Los Angeles, California 90095-1567
E-mail: win@ucla.edu

William M. Kaula

Department of Earth and Space Sciences, and Institute of Geophysics and Planetary Physics, University of California, Los Angeles, California 90095-1567

and

James M. Hyman

Theoretical Division, Los Alamos National Laboratory, Los Alamos, New Mexico 87545

We report on numerical simulations designed to understand the distribution of small bodies in the Solar System and the winnowing of planetesimals accreted from the early solar nebula. The primordial planetesimal swarm evolved in a phase space divided into regimes by separatrices which define their trajectories and fate. This sorting process is driven by the energy and angular momentum and continues to the present day. We reconsider the existence and importance of stable niches in the Jupiter/Saturn zone using highly accurate numerical techniques based on high-order optimized multistep integration schemes coupled to roundoff error minimizing methods. We repeat the investigations of W. M. Weibel *et al.* (*Icarus* **83**, 382–390, 1990) with one hundred thousand massless particles—nearly 10^3 time more particles than our 1990 investigation. Previous studies of the Jupiter/Saturn zone have employed only hundreds of particles, usually starting on circular and zero inclination orbits. By employing 10^5 particles on both inclinded and eccentric orbits, we can perform a near-exhaustive search for test particle stability as a function of initial orbital elements. The increase in the numbers of test particles also facilitates robust statistical inference and comparison with analytic results. In our simulations, we observed three stages in the planetesimal dynamics. At the start of the simulation many planetesimals are quickly eliminated by close approaches to Jupiter or Saturn. Next there is a gravitational relaxation phase where the surviving particles are exponentially eliminated by random gravitational encounters with Jupiter or Saturn. Finally, the only long-lived particles in the simulation were initially located either at a Lagrange point or in an orbit nearly commensurable with Jupiter or Saturn. We conclude that although niches for plan-etesimal material are rare, extremely high-accuracy long-duration simulations employing many particles will be able to capture even the qualitative nature of early Solar System planetesimal evolution. © 1999 Academic Press

1. INTRODUCTION

The Solar System is a paradigm for dynamical complexity that is reluctant to reveal the secrets behind its origin and evolution. Planetesimals formed from the solar nebula that accreted to form the planets underwent a winnowing according to their energy, angular momenta, and phase angles. This sorting process continues to the present day because there still exist planetesimals with marginally chaotic orbits. The dynamical phase space describing the early Solar System, as well as today's, is divided into regimes by separatrices which define the planetesimals' trajectories and fate. The Solar System we see today is the product of this dynamical complexity. The remaining planetesimals hold clues to its origin and evolution.

Observable planetesimals are absent from most candidate niches in the outer Solar System. Giorgini *et al.* (1996) have compiled a database for all Solar System bodies for which the orbits are well-determined. The solutions for the orbital elements for this database come from three sources: the Minor Planet Circulars, published by the IAU Minor Planet Center at the Harvard–Smithsonian Center for Astrophysics (Marsden 1996),

the Lowell Observatory Database of Asteroid Orbits (Bowell 1996), and the Jet Propulsion Laboratory Solar System Dynamics Group (Donald K. Yeomans, supervisor). Of the bodies from the JPL database, only 165 have semimajor axes which place them in the Jupiter/Saturn zone, and of the more than 100 asteroids in this list, all but one are Trojan asteroids—situated at the leading and trailing Lagrange points of Jupiter. The lone exception is 944 Hidalgo, which crosses the orbits of both Jupiter and Saturn. Additionally, there are also observed approximately 25 comets whose semimajor axes lie between those of Jupiter and Saturn, and all but one cross Jupiter's or Saturn's orbits, or both. This one exception, P/Schwassmann–Wachmann 1, has a semimajor axis of 6.041 AU and an eccentricity of 0.045. It is not easy to extrapolate from this one observable Jupiter/Saturn zone object to include smaller objects that would be visible had they been in the relatively nearby asteroid belt. Nevertheless, the observation of only one possibly long-lived Jupiter/Saturn object, in contrast with the order of 10,000 asteroids between Mars and Jupiter, provides a compelling observational case for assuming that the Jupiter/Saturn zone is highly depleted.

Does the apparent absence of such bodies indicate the presence of primordial processes at a time when the formation of the planets was not yet complete, or are we seeing evidence for an evolutionary process—where early Solar System bodies on the edge of chaos (Newman *et al.* 1995), exposed to qualitative bifurcations in their dynamics, were removed from all regions in the outer Solar System?

This paper and its sequel (Grazier *et al.* 1999) in which we explore the Saturn/Uranus and Uranus/Neptune zones, describe a massive simulation effort designed to unravel some of these questions. Building upon earlier work by many investigators, we seek to explore the nature of various niches situated throughout the outer Solar System. In this paper, we return to the region between Jupiter and Saturn, allowing for trajectories with nonzero inclination, to better understand the fate of material situated in this regime.

We have implemented integration methods more precise than any previously applied to this problem. Our numerical technique can be regarded as a refinement of existing methods that had been widely used by dynamicists for decades. The methods used are *exact* within double precision computer accuracy and the sole source of error is due to the cumulative effect of roundoff. In particular, our contribution to the methodology has made the accuracy formerly available only on special-purpose computers—i.e., the Digital Orrery exploited by Sussman and Wisdom (1988)—accessible to anyone with access to modern workstations. Further, we have performed the computations to minimize the accrued roundoff so that such error will not unnecessarily contaminate the outcome of our investigation. We validated our integration schemes by showing that longitude errors in the major planets grow no faster than the $t^{3/2}$, where t is the time, and the uncertainty in their positions after one billion years is less than 3°! These highly accurate simulations can be used as a benchmark against which we test other approxi-

mate integration schemes. Our integration scheme, since it is exact to machine precision, is *a posteriori* symplectic, using the definition of Feng (1987, 1995).

Thus, the first major difference between the present investigations and that of its predecessors resides in its vastly improved accuracy. The Jupiter/Saturn zone is host to numerous nearly overlapping resonances. If narrow bands of stability exist between resonances, the integration error of less accurate methods could artificially propel planetesimals on potentially stable orbits into resonant, hence unstable, orbits on time scales which are short compared to the total integration time.

This increased accuracy had the price of increased computational time, but we were able to exploit the availability of 10 high-performance Hewlett–Packard (HP) workstations in the execution of this project. Our methodology is also, to use the term commonly employed by computer scientists, "embarassingly parallel" and directly computable on the new generation of massively parallel computers.

We have performed our investigations over a period of 10^9 years, a period extending well beyond the early dynamical evolution of the Solar System. To preserve the essential physics of Solar System origin, our investigations have been fully three-dimensional and incorporate the full gravitational effect of all of the jovian planets. The effect of the terrestrial planets on the depletion of outer Solar System niches is negligible due to their small mass and high orbital frequencies—apart from their time-averaged influence—therefore we incorporated their masses into that of the Sun. Relativistic and nongravitational effects are also ignored.

Our earlier work, and that of many other groups, considered hundreds of particles in limited surveys of these niches and provided important insights into these processes. Earlier studies all suggest that the Jupiter/Saturn zone is depleted of planetesimal material on short (10^4 to 10^5 year) time scales. In previous studies, however, the coverage of phase space was modest. There could exist narrow niches of stability large enough to preserve resevoirs of particles that would go undetected by coarse surveys. One goal was to reduce the uncertainties in these initial efforts due to the "statistics of small numbers" (Newman *et al.* 1989, 1992, 1994). An essential feature to be remembered from simple random walk arguments is, for situations composed of N "events," that the prevailing uncertainty is of order $N^{1/2}$ (Chandrasekhar 1943). Accordingly, the relative uncertainty is of order $N^{-1/2}$, which requires surveys to far more than a few hundred events to be adequate for precise statistical inference.

We have employed more than 100,000 test particles in the present survey of the Jupiter/Saturn zone and, in this paper's sequel, 10,000 each in the Saturn/Uranus and Uranus/Neptune zones (Grazier *et al.* 1999). As a consequence, we are in a position for the first time to draw statistically reliable conclusions from our investigations. We felt it was important that we develop a statistical analysis based upon kinetic theory which would provide an *ab initio* confirmation of our results. We build on the theory developed by Chandrasekhar (1943) in stellar dynamics,

Spitzer (1962) in plasma physics, and Stewart and Wetherill (1988) in Solar System dynamics, incorporating the geometry of these solar system niches. Although these theories were developed for fully interacting systems, the approach proved useful in analyzing the reliability of the statistical analysis applied to the nonlinear dynamics of our approximate system.

2. PREVIOUS WORK

In 1973 Lecar and Franklin (hereafter referred to as LF73) examined the region from 5.72 to 9.10 AU for 6000 years using a model which integrated initially circular particle orbits, but modeled Jupiter and Saturn analytically. They concluded, had this region initially been populated with planetesimals, that it would quickly be depopulated—on a timescale of a few thousand years—with the possible exception of two bands at 6.8 and 7.5 AU. In the same year Everhart (1973), although primarily interested in Trojan and horseshoe orbits, used a similar model and found two potential long-life bands centered at 7.00 and 7.58 AU. While acknowledging that a far more extensive survey was required to gain insight on lifetimes, he felt it probable that no orbits in either of these bands were absolutely stable. Franklin *et al.* (1989; hereafter referred to as FLS89) extended their work from 15 years earlier and examined the lifetimes of particles with initially aligned apsidal lines and semimajor axes between 7.0 and 7.5 AU—the long-life bands from LF73 and Everhart (1973). They found that bodies with higher eccentricities, approximating those of their neighboring perturbers, had somewhat longer lifetimes than particles on more circular orbits. FLS89 concluded that it was unlikely that low-inclination bodies survived more than 10^7 years between the two planets, but noted that bodies on inclined orbits may survive somewhat longer. Duncan *et al.* (1989; hereafter referred to as DQT89) developed a two-planet mapping that approximated the restricted three-body problem and examined the zones between each of the outer planets for up to the lifetime of the Solar System (4.5 Gyr). In their model, planets were confined to circular, coplanar orbits; test particles had small eccentricities, but were similarly coplanar. Particle orbits were treated as Keplerian, except at conjunctions where they were given an impulsive perturbation and new orbital elements were calculated. Between Jupiter and Saturn, DQT89 found that all orbits became planet-crossing within 10^7 years; most were planet-crossing within 10^5 years. Finally, they noted that the "stable" bands at 6.8 and 7.5 AU from LF73 were probably unstable for durations greater than 10^6 years.

Employing a three-dimensional model in which the Sun, Jupiter, and Saturn interacted fully, Weibel *et al.* (1990; hereafter referred to as WKN90) integrated the trajectories of 125 test particles, using a sixth-order Aarseth (1972) and Ahmad and Cohen (1973) scheme. Confining their integration to low-inclination, low-eccentricity orbits in the range from 5.7 to 8.8 AU, they found that all but three particles became planet-crossers within 10^5 years (most within 10^4). WKN90 noted that the longer lived orbits tended to flank commensurabilities. They also concluded

that a truly thorough search for stable orbits in this region required a simulation with much larger ranges in eccentricity and inclinations. Using the same model as LF73, Soper *et al.* (1990) used the dynamics of the Jupiter/Saturn zone as a backdrop to test how errors in numerical accuracy can effect stable orbits. They also looked to find criteria, short of long integrations, to identify orbits which are potential planet-crossers. Using a fourth-order symplectic mapping, developed by Candy and Rozmus (1990), Gladman and Duncan (1990; hereafter referred to as GD90) integrated the trajectories of 900 particles between 6.76 and 8.06 AU. In the Gladman and Duncan survey, the Sun, Jupiter, and Saturn were mutually interacting. Theirs was the first study which used close-approach as a criteria for removing a particle from the simulation, as opposed to merely planet orbit crossing, as in previous surveys (furthermore they removed any particle leaving the Solar System)—the introduction of a close-approach criterion did not significantly affect their depletion time scale, a result paralleling FLS89. They were also the first to examine the role of nonnegligible inclinations on depletion times of particles between Jupiter and Saturn. Both the inclined and the invariable plane populations were, they observed, depleted on 10^5 year time scales. Finally, Holman and Wisdom (1993; hereafter referred to as HW93) used their symplectic mapping technique (Wisdom and Holman 1991) to survey the invariable plane for stable orbits in the range from 5 to 50 AU. The Sun, and for the first time all of the jovian planets, were fully interacting in three dimensions. All test particles were on initially circular orbits. Consistent with previous studies, the majority of their test particles between Jupiter and Saturn were eliminated on 10^4- to 10^5-year time scales (all were removed by 10^6 years).

3. NUMERICAL METHODS AND INITIAL CONDITIONS

The integration method we employ was first developed by Störmer (1907) and has a well-established pedigree among planetary astronomers. A closely related methodology was used by Cowell and Crommelin (1910) to predict the return of Comet 1P/Halley. In the mid-1960s through the early 1990s, Cowell–Störmer schemes became the standard integration methods for celestial mechanics. Concurrently and subsequently, many other astronomical and planetary dynamicists have employed this methodology.

The numerical method used in our simulations is a truncation-controlled 13th-order modified Störmer integrator which employed a roundoff error minimization technique we call "significance-ordered computation" (see Higham 1993, 1996). The accumulated integration error was as would be expected in the absence of *systematic* error in the integration scheme. We employed a time step of ≈4.24 days—sufficiently small to guarantee that the computation of any particle trajectory with eccentricity ≤0.5 was *exact* to double precision computer accuracy.

Brouwer (1937) showed that if the sole source of error of a numerical integration was due to accumulated roundoff error, which is the optimal case, then the error in energy, or "action"

type variables after n steps, should be proportional to $n^{1/2}$, while error in the corresponding "angle" type variables will vary as the integral over time of the former and should grow as $n^{3/2}$. This occurs only when all systematic sources of roundoff and truncation error are eliminated. Systematic integration error leads to energy error which grows linearly and longitude error which grows quadratically with the number of steps. Previous investigations have exhibited the hallmark of systematic error growth. Henrici (1962) also explored the role of roundoff growth in systematic and random growth environments. These scaling laws are rigorously derived in a general way in Hamiltonian action/angle variables in Goldstein (1996).

One accuracy test of our integration method was based upon integrations of the outer Solar System. For 16 different sets of initial conditions, we integrated the trajectories of the jovian planets for a time interval equivalent to 2^n Jupiter orbits, where n is an integer between 0 and 25. At the end of each integration, we use the positions and velocities of the Sun and planets as starting conditions to integrate *backward* in time. The longest of these integrations, 2^{25} Jupiter orbits both forward then backward, corresponds to a total integration time of appoximately 800 million years. This demonstrated that the integrator performed remarkably consistantly, even over very-long-duration integrations.

Figure 1 shows the relative RMS energy error for the entire system. We can see that the energy error grows as $t^{0.48}$, very nearly $t^{1/2}$, indicating the absence of systematic error growth. Figure 2 shows the RMS angular position errors for both Jupiter and Saturn. Given the initial position for a planet $\vec{r}_i$, and its final position $\vec{r}_f$, we define the angular position error λ as

$$\lambda = \arcsin\left(\frac{|\vec{r}_i \times \vec{r}_f|}{|\vec{r}_i||\vec{r}_f|}\right).$$

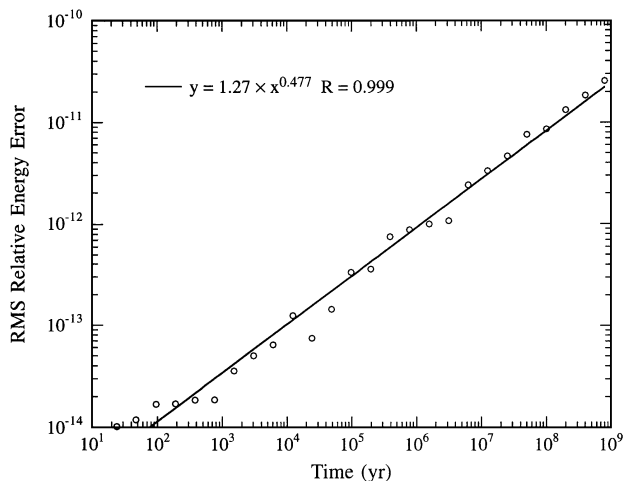If our computations had no truncation or roundoff error, we

FIG. 1. Relative RMS energy error for outer Solar System forward/back integration. Values are for times corresponding to 2^0 to 2^{25} orbits of Jupiter. Nonlinear power-law regression reveals a power law index of ≈ 0.48, indicating the absence of any significant systematic integration error.
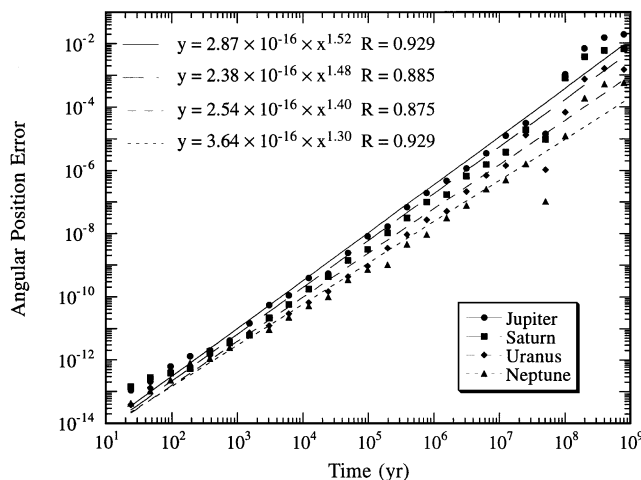

FIG. 2. Absolute RMS angular position error of the jovian planets for forward/back integrations using 16 different sets of initial conditions.

would expect that these foreward/backward integrations would yield $\vec{r}_i = \vec{r}_f$. Thus, λ is a useful measure of the accumulated error present in these calculations. In the N-body tests described in Fig. 2, we see that for all jovian planets the angular position error grows at a rate nearly equal to $t^{3/2}$. After 2^{26} Jupiter orbits (nearly 800 million years), the errors for all planets are less than of 1.9×10^{-2} radians ($\approx 1.09°$).

A detailed and mathematically rigorous development of this method and related multistep methods are in Goldstein (1996). Information and test results specific to the integrator used in this study can be found in Grazier (1997). A version of the modified Störmer integrator similar to that used in this study is available on the World Wide Web at `http://pentalith. astrobiology.ucla.edu/varadi/NBI/NBI.html`.

For our study of the Jupiter/Saturn zone, we placed one hundred thousand test particles on elliptical inclined orbits about the Sun and integrated their trajectories for up to one billion years (or until they were removed from the simulation as described below). The test particles were treated as massless and were subject to the gravitational influences of the jovian planets as well as the Sun. The Sun and planets were mutually interacting.

The code for these calculations was developed in the C language and performed on clusters of HP workstations to guarantee consistency across all the runs. Initial planetary positions and velocities were generated using JPL ephemeris DE245 (Standish, personal communication, 1994) and were identically preserved across each workstation. Each machine had a unique set of test particles whose orbital elements were randomly selected.

The test-particle semimajor axes were Gaussian distributed such that the average semimajor axis was equal to the average of Jupiter's and Saturn's, and that the 3σ points (i.e., three times the standard deviation) of the distribution were coincident with Jupiter's and Saturn's semimajor axes. Since the region of interest was the zone between Jupiter and Saturn, no initial particle semimajor axes were allowed inside 4.703 AU (Jupiter's semimajor axis minus 0.5 AU), outside 10.039 AU (Saturn's

semimajor axis plus 0.5 AU), or within either of those planets' activity spheres (Danby 1988, p. 267). The initial inclinations were similarly Gaussian distributed with an average of $0°$ and standard deviation of $10°$. (Inclinations are normally defined as being positive only. For the purpose of our initial conditions, negative inclinations are effectively the same as positive inclinations with the ascending and descending nodes interchanged.) Eccentricities were randomly chosen from 0 to 1 from an exponential distribution with an *e*-folding constant of 0.1. This means that particles with eccentricities of 0.1 occur with a $1/e$ lower frequency as those with eccentricities of 0.0, and so on. The initial phase angles, longitudes of nodes, and longitudes of perihelia were randomly selected from a uniform distribution between 0 and 2π. Random number generation was performed using procedures (`RAN2`, `EXPDEV`, and `GASDEV`) from Press *et al.* (1988).

Input/output was done in heliocentric coordinates while the integrations were performed in a barycentric frame. The latter provided us with an additional accuracy check on the system center of mass' position and velocity.

In this simulation, a test particle was considered to be eliminated if it met one of three criteria: (a) Particles were removed from consideration if they underwent a close-encounter and passed within the activity sphere of a planet. Here, we used the modified definition of activity radius from Holman and Wisdom (1993), namely

$$r_{act} = a_0 \left(\frac{m_p}{M_\odot} \right)^{2/5},$$

where m_p is the mass of a given planet, and a_0 its initial semimajor axis. (b) A particle was considered ejected from the Solar System, and thus removed from the simulation, if (1) it had positive energy relative to the Sun and all of the planets, (2) it had heliocentric radius greater than 50.0 AU, and (3) the projection of its velocity against a radial line from the Sun was positive, i.e., was on an outbound trajectory with $\vec{r} \cdot \vec{v} > 0$. We included the third ejection criterion because we recognized the possibility, albeit small, that an incoming particle on a hyperbolic (unbound) orbit could, through planetary interactions, lose energy and subsequently become rebound (Everhart 1968). (c) If a particle came within 1 AU of the Sun, we calculated its perihelion distance. If this was less than R_{Sun}, then the particle was eliminated from the simulation. It should be noted that throughout the entire 100,000 particle simulation, no such "Sungrazers" (Levison and Duncan 1994) were detected, despite the additional mass of the inner planets being added to that of the Sun.

4. RESULTS

As is often the case when exploring a new problem (or an old one using refined tools), the initial phase of our data analysis was exploratory—to try to identify the different periods of evolution and the relevant physics. The physical ingredient that
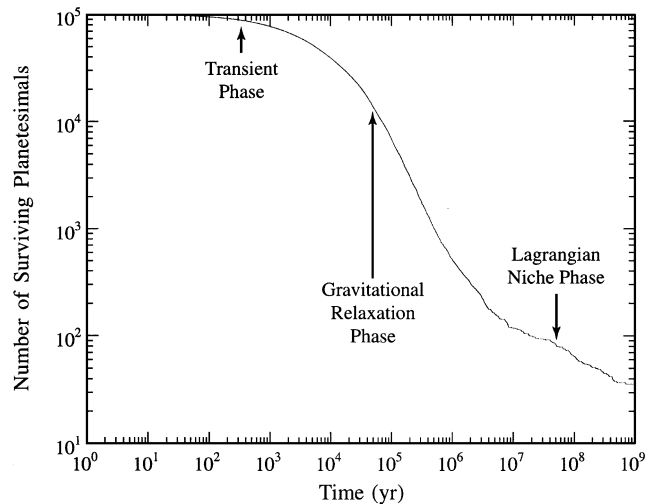

FIG. 3. Plot of number of surviving particles in our simulation as a function of time. From this, we can clearly see that the evolution occurs in three phases.

we believe must be central to this problem is kinetic theory. In Fig. 3, we plot the number of surviving planetesimals as a function of time. We observe that there are three basic evolutionary periods in this problem, unlike HW93 who found that the number of planetesimals as a function of time followed a $1/t$ dependence, with t being the run time. This is possibly explained by the different initial conditions used in each study. First, there is a transient phase associated with the start of the simulation where many planetesimals are quickly eliminated by either the activity spheres of Jupiter and Saturn or by virtue of being on very eccentric, even planet-crossing, orbits from the beginning. Second, there is a gravitational relaxation phase where the surviving particles undergo a random walk in momentum space, being scattered successively by gravitational encounters from the planets until they are eliminated after interacting with an activity sphere. (If we had displayed the results in log-linear fashion, we would see an essentially exponential decay during this phase where the *e*-folding time evolves upward as the winnowing proceeds.) Finally, there is a phase characterized by long-lived particles that reside either in the neighborhood of stable Lagrangian points or, albeit less often, in candidate stable niches (often flanking commensurabilities).

We have obtained estimates of the *e*-folding time scales appropriate using a nonlinear exponential fit to the different time ranges. During the first phase, extending from the time origin to 3×10^3 years, the *e*-folding time was observed to be $\approx 6.8 \times 10^3$ years. During the gravitational relaxation phase, from 10^5 to 5×10^5 years, the *e*-folding time was observed to be $\approx 2.0 \times 10^5$ years. Finally, during the "Lagrangian niche" phase, from 10^7 years on, the *e*-folding time has become extremely long, of order 2×10^8 years.

In Fig. 4, we provide an illustration that describes how this situation unfolds. We show a Gaussian, signifying the planetesimal swarm's initial distribution in semimajor axis, flanked by the activity spheres of Jupiter and Saturn. With the initiation of
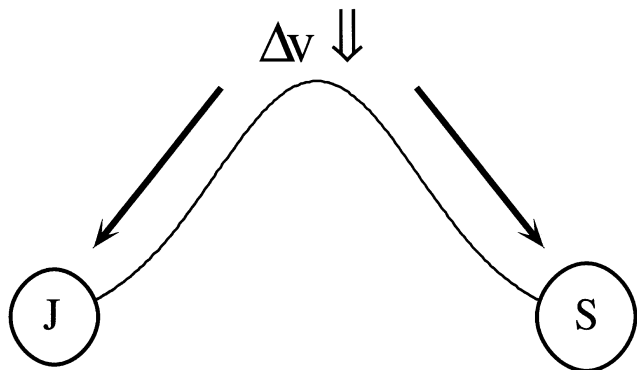
FIG. 4. An idealized representation of the time evolution of the particles in the Jupiter/Saturn zone. The Gaussian curve represents our initial particle distribution in semimajor axis, whereas the spheres at the wings represent the activity spheres of the two planets. The maximum Δv occurs near the peak of the initial particle distribution. As the wings of the distribution are depleted, they are replenished from the inside out by the planetesimals' random walk in momentum space.

the simulation, many of the planetesimals will have trajectories that quickly bring them into the path swept up by the activity spheres of Jupiter and Saturn. This is in agreement with the observations of FLS89 where there was a 2 to 6% difference between the time a particle's orbit became planet crossing and entry into a close-approach. It is appropriate to describe this initiation phase as a collision of "hard spheres" with the point planetesimal particles. This aspect of kinetic theory was first developed by Chapman and Enskog and is clearly described in the text by Chapman and Cowling (1970): the collision frequency v varies as $n\sigma \Delta v$ where n is the number density of colliders (i.e., Jupiter and Saturn), σ is the "collision cross section" of the collider, namely πR^2 where R is the radius ≈ 0.34 AU of the two activity spheres, and Δv is a measure of the velocity difference between planetesimal and planet. The number density is estimated from the volume appropriate to our initial planetesimal distribution (see above) and has the form of a torus extending between the orbits of Jupiter and Saturn, and subtending an angle normal to the invariable plane with respect to the Sun of $\approx 20°$. We took the corresponding volume to be ≈ 516 AU^3. Since the circular velocity $v \propto a^{-1/2}$, we estimated the differential velocity Δv according to the velocity difference between a planet at the center of an activity sphere and a planetesimal at its periphery, hence $\Delta v \approx (\Delta a/2a)v$. For Jupiter, we obtained $\Delta v \approx 8.4 \times 10^{-2}$ AU/year (with a slightly smaller value for Saturn). Putting these quantities together yields an approximate time scale, i.e., the reciprocal of v, of 8.2×10^3 years, in close agreement with our fit to the data shown in Fig. 3.

The important point illustrated by Fig. 4 relates to the gravitationally dominated phase of evolution when planetesimals undergo a form of random walk in momentum space, undergoing intermittent gravitational boosts as they wend their way among the jovian planets. There is a time scale associated with this process which describes the length of time required for a

particle to undergo a major deflection by a planet. The process of gravitational relaxation was first developed by Chandrasekhar (1943) and was elaborated upon in a major way for general Coulomb interactions by Spitzer (1962). For more up-to-date treatments including significant improvements in the treatment of gravitational interactions in a planetesimal swarm in the context of Solar System dynamics, see Stewart and Kaula (1980) and Stewart and Wetherill (1988).

Figure 4 reminds us that Δv is greatest at the center of the Gaussian distribution and diminishes as the particle draws near to a jovian planet. We can employ the Virial Theorem to relate Δv to the effective interaction distance r between a planetesimal and a planet of mass M, namely $GM/r \approx \Delta v^2$. Accordingly, we replace the "hard sphere" cross section σ introduced above by the velocity-dependent version $\sigma_{\Delta v}$ according to $\pi r^2 \approx \pi (GM/\Delta v^2)^2$. Then, the appropriate time scale τ varies as $\Delta v^3/\pi n(GM)^2$. This expression shows us that gravitational collision times are smallest when Δv is smallest. Hence, planetesimals which closely flank the activity spheres are among the first to be deflected into the path of these spheres of influence. Planetesimal material closer to the center of the Gaussian distribution in Fig. 4 requires much more time to complete its random walk into the path of a moving activity sphere. The time scale appropriate to the minimum relevant Δv is, in fact, approximately the same as that which we derived for the activity sphere. That should be no surprise since the activity spheres describe a form of force or virial balance. What is more instructive is to estimate the lifetime of those particles which must undergo the greatest change in Δv. For these longest lived particles, Δv is simply the differential velocity between the orbits of Jupiter and Saturn, or about 0.95 AU/year. Since we wish to consider gravitational scattering by either Jupiter or Saturn, we will employ the geometric mean of their GM values, or 2.06×10^{-2} AU^3/year^2. We obtain, therefore, a gravitational relaxation time scale 1.7×10^5 year, in close agreement with our empirical value of 2.0×10^5 year. Thus, a simple kinetic theory and ideas from the statistical mechanics of particulate systems and the Coulomb force permits us to derive theoretically some of the basic features of our simulations!

Our discussion of kinetic theory has ignored the roles of Uranus and Neptune, which have a relatively modest influence on planetesimal evolution. Basically, the outer jovian planets can affect only those planetesimals whose semimajor axes and/or eccentricities have been pumped up so as to come within their range of influence. Elementary kinetic theory is inadequate in predicting the singular gravitational events that can propel planetesimals into their spheres of influence of Uranus and Neptune. We also expect that our statistical approach will perform best when the neighboring perturbers are of a similar (within an order of magnitude) size. It should also perform better when the perturbers are more closely spaced.

It is important to note that the evolution of the Solar System on time scales long compared to 10^5 years is dominated by effects, such as resonances, not describable by simple kinetic theory. In

fact the evolution of particles in our Jupiter/Saturn zone study was more complex than the simplified diagram in Fig. 4, as resonances manifested on much shorter than 10^5-year time scales. In Fig. 5 we have plotted the number of surviving particles as a function of *initial* semimajor axis for times ranging from the beginning of the simulation up to 2×10^5 years. The orbits of many particles will have certainly been altered over time, nevertheless this plot provides valuable insight into the evolution of the Jupiter/Saturn zone. We clearly see two important points. First, we see that unmistakable trend of a symmetric winnowing of planetesimals from the vicinity of Jupiter and Saturn into the heart of the Jupiter/Saturn zone did occur, similar to our description in Fig. 4. Additionally, we also see that particles initially situated in the vicinity of 7.3 AU are rapidly depleted due to the Jupiter 3 : 5 and Saturn 3 : 2 mean motion commensurabilities. Figure 5 confirms the observations of LF73, Everhart (1973), and FLS89 that particles in the bands near 7.0 and 7.5 AU have much longer lifetimes than particles situated elsewhere in the Jupiter/Saturn zone.

Figure 6 shows the minimum and maximum lifetimes of particles in our simulation as a function of their initial semimajor axis range in 0.1-AU semimajor axis intervals. Note the features from 5.0 to 5.3 AU and from 9.3 to 9.6 AU. These correspond to particles librating in Trojan, "horseshoe," or "tadpole" orbits with respect to Jupiter and Saturn, respectively. Only 65 particles of the original 10^5 survived the first 100 million years integration. Of these, 57 were in Trojan orbits, 7 were coorbiting with Saturn (termed "Bruins" by de la Barre *et al.* 1996), and 1 was situated at 6.6 AU. All long-lived particles in Trojan orbits began their lives there and did not arrive at these niches as a result of dynamical evolution. All of the Saturn coorbiters were removed from the simulation by 366 Myr, while 35 Trojans survived the entire one-billion-year integration.
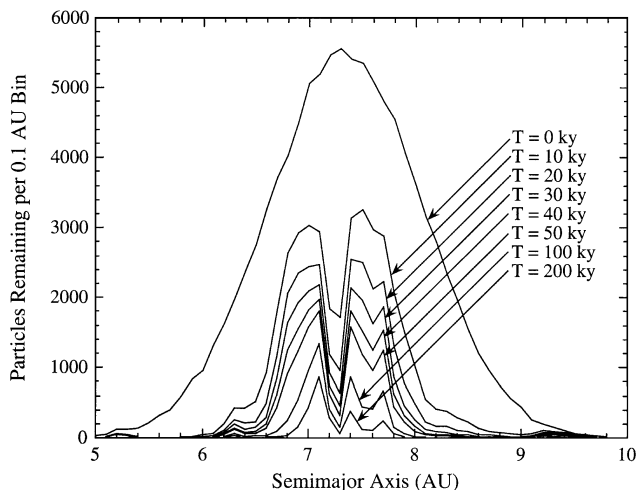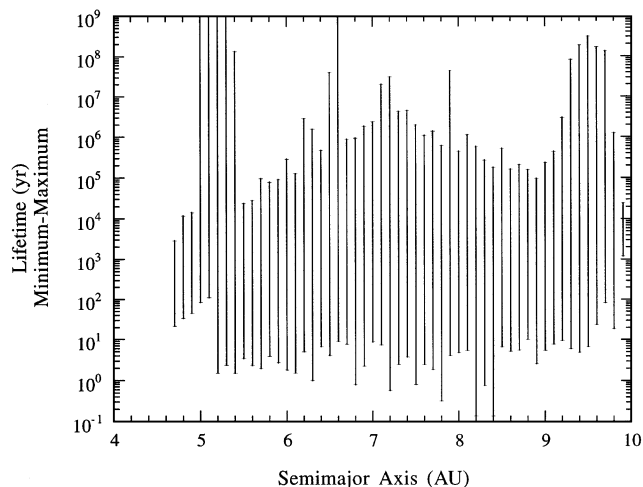

FIG. 6. Minimum and maximum lifetimes as a function of initial semimajor axis range in 0.1-AU intervals. Spikes at 5.2 and 9.5 AU correspond to Jupiter and Saturn librators.

The plot of maximum and minimum lifetimes in Fig. 6 contains only limited information. The maximum lifetimes often represent the duration of the simulation in contrast with the time spent in the Jupiter/Saturn zone. As an example, one particle with an initial semimajor axis of 7.9 AU achieved a semimajor axis of 109,000 AU (corresponding to a period of approximately 3.6×10^7 years) but nevertheless remained bound to the Solar System. On its next passage through the Solar System, its orbit was perturbed and it was subsequently classified as ejected. The fact that this lone particle survived so long in the simulation before meeting our criteria for elimination is another indication that the maximum lifetimes can be misleading. Similarly, all minimum-lifetime particles for each range were relatively eccentric and often were on planet-crossing orbits from the onset of the simulation. In short, maximum and minimum value statistics can be misleading. In simulations with orders of magnitudes fewer particles, such a plot of particle lifetimes yields primarily maximum/minimum value statistics.

A much more informative measure of the expected lifetimes of particles in the Jupiter/Saturn zone is shown in Fig. 7. Here we considered the lifetime distribution in each semimajor axis interval and identified the first and third interquartile ranges, namely the times below which 25 and 75%, respectively, of the planetesimals had been eliminated. (Another measure of statistical variability could have been produced by plotting the mean lifetime with "error bars" denoting one standard deviation.) Again, we see strong features at 5.2 and 5.3 AU corresponding to Trojan orbits, but the analogous features for Saturn coorbiters have sharply decreased in magnitude. Also note the depression at 7.3 AU, corresponding to the Saturn 3 : 2 mean motion resonance and the Jupiter 3 : 5 resonance.

It should be pointed out that the depletion and expected lifetimes we see in Figs. 4 and 7 are those for a non-self-gravitating disk. Work done by Ward and Hahn (1997) indicates that in

FIG. 5. The number of surviving planetesimals as a function of time and initial semimajor axis range. We see both a symmetric outward/in winnowing as well as rapid depletion from the region near 7.3 AU, corresponding to the Jupiter 3 : 5 and Saturn 3 : 2 mean motion commensurabilities.
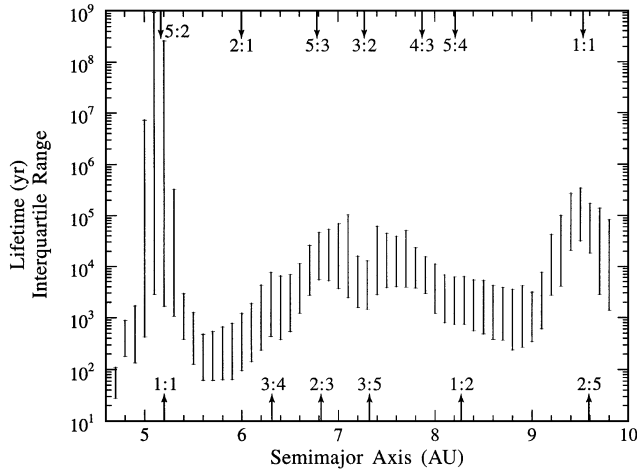
FIG. 7. Similar to Fig. 6., particles were grouped according to initial semimajor axis in 0.1-AU intervals and sorted with respect to their lifetimes. High and low values represent the first and third quartiles, respectively. With the exception of the Jupiter and Saturn librators, 75% of the particles are eliminated within 10^5 years, in agreement with previous studies. Jupiter commensurabilities are indicated across the bottom of the figure and Saturn commensurabilities across the top.

the presence of a self-gravitating disk, collective behavior of gravitationally interacting and colliding particles may manifest. Eccentricities which may have been "pumped up" for particles in low-order mean motion resonances with the jovian planets may therefore become damped. This implies that the expected lifetimes in a self-gravitating disk would be longer than those presented here.

On the other hand, the expected lifetimes we see in Fig. 7 are valid for particles in a highly depleted Jupiter/Saturn zone— that which we see today. In the Introduction of this paper we noted that observationally there is only one body on a nearly circular orbit between Jupiter and Saturn: comet P/Schwassman–Wachmann 1 with a semimajor axis of 6.041 AU. From Fig. 5, we examine the first and third quartiles of the planetesimal in the corresponding bin and see that the expected lifetime for a body between 6.0 and 6.1 AU is on the order of 10's to less than 10^3 years. The implications from our simulation is that this body is a short-time resident of its present orbit; it arrived as a result of dynamical evolution and will be perturbed out of its present orbit on a very short time scale (Grazier *et al.* 1998).

Although it was one particle out of 100,000, we were curious about the conditions under which the particle at 6.6 AU remained stable and relatively unchanged throughout the entire 10^9-year integration. We therefore performed a 2000-particle targeted search of the region surrounding it. All distributions of orbital elements were the same as those described earlier, with the exception of a semimajor axis which was uniformly distributed between 6.4 and 6.8 AU. No particle in this subsequent search survived more than 2.6 million years.

Table I provides an indication of the relative significance of various mechanisms for depleting planetesimals from different semimajor axis ranges. In each 0.1-AU interval we indicate how

TABLE I
Method of Termination in the Simulation as a Function of Initial Semimajor Axis

Axis	Alive	Jupiter	Saturn	Uranus	Neptune	Eject
4.7	0	9	0	0	0	0
4.8	0	14	1	0	0	0
4.9	0	22	1	0	0	0
5.0	0	22	0	0	0	0
5.1	4	33	1	1	0	0
5.2	25	65	1	0	0	0
5.3	6	99	1	0	0	0
5.4	0	141	4	0	0	0
5.5	0	201	8	0	0	0
5.6	0	308	6	0	0	0
5.7	0	375	20	0	0	0
5.8	0	528	45	0	0	0
5.9	0	744	93	4	0	1
6.0	0	851	106	2	1	0
6.1	0	1,083	229	4	2	1
6.2	0	1,255	358	5	1	0
6.3	0	1,444	530	11	0	3
6.4	0	1,554	812	5	4	2
6.5	0	1,667	1,068	16	7	3
6.6	1	1,745	1,501	14	8	0
6.7	0	1,855	1,837	18	3	2
6.8	0	1,916	2,089	8	11	4
6.9	0	2,040	2,431	27	7	2
7.0	0	2,100	2,918	35	7	3
7.1	0	2,164	2,973	34	9	3
7.2	0	2,281	3,155	17	10	4
7.3	0	2,141	3,377	33	7	3
7.4	0	1,816	3,555	33	8	2
7.5	0	1,528	3,791	31	4	2
7.6	0	1,543	3,495	23	11	1
7.7	0	1,326	3,438	24	4	1
7.8	0	1,133	3,392	14	5	3
7.9	0	937	3,102	21	5	4
8.0	0	702	2,892	24	4	0
8.1	0	475	2,647	18	6	1
8.2	0	413	2,364	10	0	1
8.3	0	335	1,989	9	2	0
8.4	0	266	1,677	10	2	0
8.5	0	197	1,336	9	2	1
8.6	0	140	1,048	3	0	0
8.7	0	84	864	4	0	0
8.8	0	55	679	5	0	0
8.9	0	46	507	3	0	1
9.0	0	30	409	3	1	0
9.1	0	12	251	2	0	0
9.2	0	11	192	0	0	0
9.3	0	4	146	2	0	0
9.4	0	6	84	0	0	0
9.5	0	5	60	0	0	0
9.6	0	0	38	0	0	0
9.7	0	5	30	0	0	0
9.8	0	1	13	0	0	0
9.9	0	1	9	0	0	0
10.0	0	0	2	0	0	0
Totals	36	37,728	61,575	482	131	48

many particles presently remain, how many were eliminated by the activity spheres of Jupiter, Saturn, Uranus, and Neptune, respectively, and how many were ejected from the Solar System. (Importantly, no planetesimals were eliminated by the "Sun-grazing" criteria.) Here, direct comparisons with the results of other researchers are difficult because (1) our simulation was not confined to the invariable plane as were most of the others, (2) our simulation was not limited solely to Keplerian jovian planetary orbits, and (3) the much smaller number of particles employed in previous surveys renders such counts more susceptible to the "statistics of small numbers" (Newman *et al.* 1992). Importantly, we note that we can make statistically valid inferences about the significance of various mechanisms, since the relative uncertainty in our results varies as O ($N^{-1/2}$).

Uranus and Neptune together eliminate about 1/2% of the planetesimals. Of our 10^5 planetesimals, only 48 were ejected from the Solar System. HW93, however, observed "no non-elliptic orbits were detected before close encounter." It is entirely possible that this is an outcome of the relatively small sample size which they employed or the fact that our intial distribution contained some particles initially on fairly eccentric orbits.

GD90 noted that for particles in the plane, close approaches with Saturn were more numerous than those with Jupiter by a ratio of $266/175 \approx 1.520$, while for the inclined population, the roles were reversed and close approaches with Jupiter occurred $223/182 \approx 1.226$ times more frequently—we give their observed populations as a possible indication of the role of the statistics of small numbers. They attributed this role reversal to the fact that "inclined particles are typically further from the plane near Saturn than near Jupiter and therefore less likely to have encounters." Because all the particles must eventually pass through the plane, we investigated this. We grouped our 10^5 particle distribution in $1°$ inclination intervals and display the numbers removed by the various available mechanisms in Table II. These "mechanisms" include, as in Table I, the four jovian planets and Solar System ejection, as well as show what number of planetesimals survived 10^9 years. What is particularly noteworthy is the relative effectiveness of Saturn's activity sphere eliminating planetesimals in contrast with Jupiter's. Geometric and dynamic intuition would imply that planetesimals on highly inclined orbits will be less likely to deviate from their respective courses than planetesimals traveling in the plane—the odds for mutual avoidance become much greater for planetesimals with highly inclined trajectories; also, it is more difficult to change the direction of the angular momentum vector than its magnitude. Another element of geometric intuition emerges when we consider the relative importance of planetesimal deflection by Jupiter or by Saturn. We show in Table II, that particles of all inclinations tended to have more frequent close approaches with Saturn. The relative number of planetesimals swept away by the activity spheres of Jupiter and Saturn (which have essentially the same radius) should vary as the ratio of the areas of the two annuli swept out by these two jovian planets, a ratio of approximately $1.0 : 1.9$—this presupposes a "symmetric" initial distribution be-

TABLE II
Method of Termination in the Simulation as a Function of Initial Inclination

Inclination	Alive	Jupiter	Saturn	S : J Ratio	Uranus	Neptune	Eject
$0 \leq i < 1$	2	2,865	5,107	1.78	24	6	0
$1 \leq i < 2$	1	2,800	5,148	1.84	16	5	0
$2 \leq i < 3$	4	2,914	4,631	1.59	32	3	1
$3 \leq i < 4$	3	3,021	4,497	1.49	45	10	3
$4 \leq i < 5$	3	2,932	4,269	1.46	37	7	3
$5 \leq i < 6$	7	2,782	3,991	1.43	44	19	1
$6 \leq i < 7$	3	2,554	3,841	1.50	37	10	2
$7 \leq i < 8$	3	2,280	3,578	1.57	47	7	3
$8 \leq i < 9$	0	2,155	3,412	1.58	26	14	10
$9 \leq i < 10$	3	1,879	3,130	1.67	30	11	2
$10 \leq i < 11$	2	1,755	2,833	1.61	24	6	3
$11 \leq i < 12$	1	1,602	2,609	1.63	25	5	5
$12 \leq i < 13$	2	1,238	2,244	1.81	17	6	2
$13 \leq i < 14$	0	1,155	2,036	1.76	23	7	5
$14 \leq i < 15$	0	980	1,790	1.83	12	5	3
$15 \leq i < 16$	0	840	1,634	1.95	12	0	2
$16 \leq i < 17$	0	719	1,280	1.78	9	3	1
$17 \leq i < 18$	1	645	1,053	1.64	9	1	0
$18 \leq i < 19$	1	495	863	1.74	2	2	0
$19 \leq i < 20$	0	431	712	1.65	1	2	1
$20 \leq i < 21$	0	329	612	1.86	2	0	1
$21 \leq i < 22$	0	272	514	—	2	1	0
$22 \leq i < 23$	0	245	427	—	3	0	0
$23 \leq i < 24$	0	202	320	—	1	0	0
$24 \leq i < 25$	0	144	260	—	0	0	0
$25 \leq i < 26$	0	114	217	—	1	1	0
$26 \leq i < 27$	0	103	152	—	1	0	0
$27 \leq i < 28$	0	75	117	—	0	0	0
$28 \leq i < 29$	0	46	67	—	0	0	0
$29 \leq i < 30$	0	40	45	—	0	0	0
$30 \leq i < 90$	0	116	186	—	0	0	0
Totals	36	37,728	61,575	—	482	131	48

Note. We also note the ratio of the number of terminations by Jupiter compared to those of Saturn (until the number of particles in the range drops below 1000 and we can no longer make statistically meaningful inferences). These values are in relatively good agreement with the ratio 1.9 : 1 which we derive in the text.

tween them. This is an additional feature we should look for in our simulation: the expectation, from the geometry the annuli swept out and kinetic theory, that Saturn would appear to be 1.9 times more effective at eliminating planetesimals than Jupiter. The column in Table II denoted "S : J Ratio" shows that this proportion remains near 1.9, never descending to 1.0. (We do not display this ratio, although it remains consistent with our prediction, when the total planetesimal count in a given inclination region drops below 1000 as it would become overly sensitive to the small population.)

GD90 reported that particles with nonzero inclinations began to be removed *later* in the simulation than those in the invariable plane, but that once planetesimal removal began in the plane it would proceed at a faster pace. After approximately 20,000 years, GD90 found that the fraction of remaining particles was the same independent of initial inclination. Figure 8
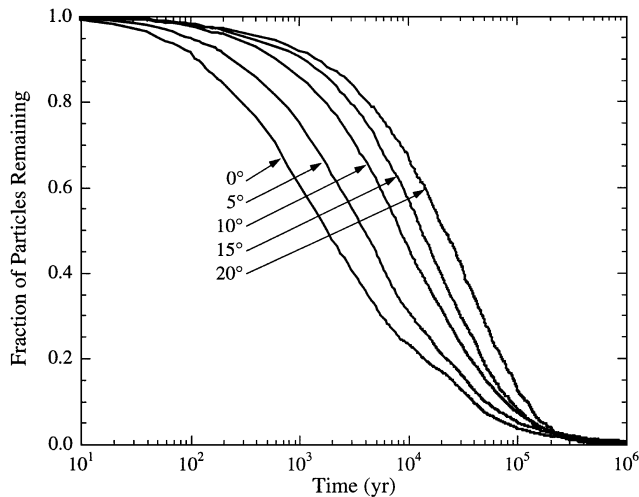
FIG. 8. Fraction of remaining particles as a function of time for inclinations of 0, 5, 10, 15, and 20 degrees. Each curve represents particles with initial inclinations which fall within ±0.5 degrees of the aforementioned values. On short time scales, inclination has a marked effect on lifetimes.

shows a family of curves displaying the relative depopulation of the planetesimal swarm as a function of initial inclination starting at 0° and varying in 5° increments up to 20°. In agreement with GD90, we clearly see that early in the simulation, particles with lower inclinations are removed more quickly.

Analogous to Fig. 8, Fig. 9 provides a family of curves that show removal rates as a function of eccentricity. We observe that more eccentric orbits have markedly shorter lifetimes than less eccentric ones, as we would intuitively expect. The essential
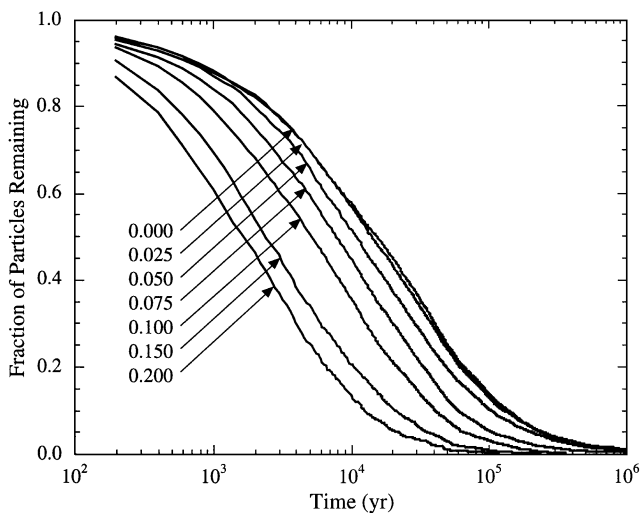
feature here is that, as time proceeds, highly eccentric particles are the first to disappear and we are left with a population of particles with ever-decreasing eccentricities. FLS89 suggested that more eccentric particles might be somewhat more stable if their eccentricity approximated that of the perturbers. Looking at the removal curve for $e = 0.05$ (where, for Jupiter, $e = 0.048$ and, for Saturn, $e = 0.056$), we see no indication of this. It is possible that the use of initial conditions with aligned apsides may produce a situation where increasing the eccentricity further increases the stability, well beyond that characteristic of planetary orbits.

Tables III and IV describe an outward migration of planetesimals in the simulation—a feature alluded to in Table I. Table III shows the final semimajor axis range for all 100,000 particles at the end of 100 Myr simulation time. Over 11% of the particles had their final semimajor axes outside of that of Saturn at the end of the simulation; 48 were completely ejected from the solar system. Less than 2% of the particles were injected into the inner Solar System. Even within the Jupiter/Saturn zone, the trend was for the particles to move outward—this can be seen in Table IV. Table IV shows the initial and final semimajor axes (and standard deviations) for the sample of particles eliminated by collision with the activity sphere of each planet. The average semimajor axes of the particles eliminated by *every* planet indicate that the trend was for the particles to migrate outward, with their orbits becoming increasingly eccentric in the process.

FIG. 9. Similar to Fig. 8, each curve represents the fraction of particles remaining with initial eccentricities falling within ±0.005 of 0.025, 0.050, 0.075, 0.100, 0.150, and 0.200. The highly eccentric particles are eliminated more rapidly. This is true even of those with initial eccentricities of 0.05, which, it had been previously suggested, may be longer lived by virtue of being close in eccentricity to that of their neighboring planets.

TABLE III

Initial and Final Mean Semimajor Axes, as well as Standard Deviations, for All Planetesimals

Final semimajor axis (by category)	Number in range
$a < 4.7$	1,688
$4.7 \leq a < 10.03$	87,068
$10.03 \leq a < 15$	9,804
$15 \leq a < 20$	916
$20 \leq a < 25$	227
$25 \leq a < 30$	93
$30 \leq a < 40$	74
$40 \leq a < 50$	39
$50 \leq a < 60$	12
$60 \leq a < 70$	7
$70 \leq a < 80$	5
$80 \leq a < 90$	2
$90 \leq a < 100$	3
$100 \leq a < 200$	4
$200 \leq a$	10
Ejected	48
Total	100,000

Note. Particles are grouped according to which planet's activity sphere was ultimately responsible for their removal from the simulation. Note that, in all cases, the mean final semimajor axes are greater than the initial, indicating a general outward migration.

TABLE IV
Final Semimajor Axis Ranges for All Particles at the Time of Their Removal from the Simulation

Planet (AU)	Planetary distance	Planetesimal mean		Planetesimal SD	
		Initial	Final	Initial	Final
Jupiter	5.203	7.028	7.306	0.384	4.790
Saturn	9.539	7.616	8.867	0.353	6.885
Uranus	19.18	7.449	15.567	0.362	5.148
Neptune	30.06	7.300	23.402	0.578	7.967

Note. Approximately 2% of the planetesimals reside in the inner Solar System at the time of their termination, while over 11% migrate into the outer Solar System, or well beyond.

Even particles eliminated by Jupiter had, on average, semimajor axes greater than that with which they began the simulation.

Dynamical effects governing mixed populations of "heavy" and "light" self-gravitating particles over very long periods of time have been a subject of investigation, especially in galactic dynamics, for many years. Overwhelming evidence has emerged that a "mass segregation effect" occurs where the heavy particles shed energy and angular momentum, thereby gravitating inward, while the lighter particles gain both energy and angular momentum causing them to move outward (Farouki and Salpeter 1982; Farouki *et al.* 1983; Spitzer 1987; Stewart and Wetherill 1988), sometimes being ejected from the system. This mass segregation phenomenon became widely used as an empirical diagnostic for the reliability of N-body galactic dynamics codes. Since the planetesimals we modeled were massless, they had no effect upon evolution of the planets. However, we believe that Tables I, III, and IV indicate that our system at least partially exhibited the mass segregation phenomenon and that we see that the particles tended to migrate outward.

Apart from Jupiter and Saturn coorbiters, only one particle, at 6.6 AU, survived the integration—with its semimajor axis virtually unchanged—for one billion years while retaining a small eccentricity (≤ 0.075) and inclination ($< 0.35°$). In the Introduction of this paper, we noted that the Jupiter/Saturn zone appears to be vastly depleted of planetesimal material—the interesting execptions being the Trojan Asteroids and comet P/Schwassmann–Wachmann 1, which is on a fairly circular ($e = 0.045$) orbit. It is amusing, then, that at the end of 10^9 years we are left with a simulated Jupiter/Saturn zone which looks very much like observable one: a batch of Trojans, and one particle on a nearly circular orbit.

5. CONCLUSIONS

Our investigation of the Jupiter/Saturn zone has employed the most accurate numerical techniques ever brought to bear on this class of problems and employed nearly 10^3 times as many test particles than any previous study. We have derived and applied a statistical methodology based upon kinetic theory to analyze the reliability of the relevant quantitative results.

The outcome of this study that is relevant to our Solar System's origin is that niches for planetesimal material will be few and far between. The primordial planetesimal swarm resided in a phase space divided into regimes by separatrices which define their trajectories and fate. The Lagrange points (the Trojans of Jupiter and the Bruins of Saturn), possibly some highly inclined and/or eccentric (i.e., Hilda group) orbits, plus conceivably a few nearly commensurable regions in the Jupiter/Saturn zones, will remain stable over a significant fraction of the age of the Solar System. For the overwhelming bulk of this material, it appears that we are seeing evidence for an evolutionary process, where early Solar System material was removed from almost all regions in the Jupiter/Saturn zone.

REFERENCES

Aarseth, S. J. 1972. Direct integration methods of the N-body problem. In *Gravitational N-body Problems* (M. Lecar, Ed.), IAU Colloquium No. 10, pp. 29–43. Reidel, Dordrecht.

Ahmad, A., and L. Cohen 1973. A numerical integration scheme for the N-body gravitational problem. *J. Comput. Phys.* **12**, 389–402.

Bowell, E. L. G. 1996. The Asteroid Orbital Element Database, ftp.lowell.edu/pub/elgb/astorb.html (28 October 1996).

Candy, J., and W. Rozmus 1990. A symplectic integration algorithm for separable Hamiltonian functions. *J. Comput. Phys.* **92**, 230–256.

Chandrasekhar, S. 1943. *Principles of Stellar Dynamics*. Univ. of Chicago Press, Chicago.

Chapman, S., and T. G. Cowling 1970. *The Mathematical Theory of Nonuniform Gases*, 3rd ed. Cambridge Univ. Press, Cambridge, UK.

Cowell, P. H., and A. C. D. Crommelin 1910. Investigations of the motion of Halley's comet from 1759 to 1910. In *Greenwich Observations for 1909*. Neill, Bellevue, England.

Danby, J. M. A. 1988. *Fundamentals of Celestial Mechanics*, 2nd ed. Willmann-Bell, Richmond, VA.

de la Barre, C. M., W. M. Kaula, and F. Varadi 1996. A study of orbits near Saturn's triangular lagrangian points. *Icarus* **121**, 88–113.

Duncan, M., T. Quinn, and S. Tremaine 1989. The long-term evolution of orbits in the Solar System: A mapping approach. *Icarus* **82**, 402–418.

Everhart, E. 1968. Change in total energy of comets passing through the Solar System. *Astron. J.* **73**, 1039–1052.

Everhart, E. 1973. Horseshoe and Trojan orbits associated with Jupiter and Saturn. *Astron. J.* **78**, 316–328.

Farouki, R. T., and E. E. Salpeter 1982. Mass segregation, relaxation, and the Coulomb logarithm in N-body systems. *Astrophys. J.* **253**, 512–519.

Farouki, R. T., G. L. Hoffman, and E. E. Salpeter 1983. The collapse and violent relaxation of *N*-body systems: Mass segregation and the secondary maximum. *Astrophys. J.* **271**, 11–21.

Feng, K., and M. Z. Qin 1987. The symplectic methods for the computation of Hamiltonian equations. In *Proc. Conf. Num. Methods PDE's*, pp. 1–37. Springer-Verlag, Berlin.

Feng, K., and M. Z. Qin 1995. The step-transition operators for multistep methods of ODE's. In *Feng Kang's Collected Works, Volume II*. Available at http://lsec.cc.ac.cn/disk2/ftp/pub/FENGKang/fkp.html.

Franklin, F., M. Lecar, and P. Soper 1989. Original distribution of the asteroids. II. Do stable orbits exist between Jupiter and Saturn? *Icarus* **79**, 223–227.

Giorgini, J. D., D. K. Yeomans, A. B. Chamberlin, P. W. Chodas, R. A. Jacobsen, M. S. Keesey, J. H. Lieske, S. J. Ostro, E. M. Standish, and R. N. Wimberly, 1996. JPL's on-line Solar System data service. *Bull. Am. Astron. Soc.* **29**, 1099.

Gladman, B., and M. Duncan 1990. On the fates of minor bodies in the outer Solar System. *Astron. J.* **100**, 1680–1693.

Goldstein, D. 1996. *The Near-Optimality of Störmer Methods for Long Time Integrations of $y'' = g(y)$*. Ph.D. dissertation, Department of Mathematics, Univ. of California, Los Angeles.

Grazier, K. R. 1997. *The Stability of Planetesimal Niches in the Outer Solar System: A Numerical Investigation.* Ph.D. dissertation, Department of Earth and Space Sciences, Univ. of California, Los Angeles.

Grazier, K. R., A. B. Chamberlin, and W. I. Newman 1998. Close approach modeling and the fate of 29P/Schwassmann–Wachman 1. *Bull. Am. Astron. Soc.* **30**, 1143.

Grazier, K. R., W. I. Newman, F. Varadi, W. M. Kaula, and J. M. Hyman 1999. Dynamical evolution of planetesimals in the outer Solar System. II. The Saturn/Uranus and Uranus/Neptune zones. *Icarus* **140**, 353–368.

Henrici, P. 1962. *Discrete Variable Methods in Ordinary Differential Equations*. Wiley, New York.

Higham, N. J. 1993. The accuracy of floating point summation. *SIAM J. Sci. Comput.* **14**, 783–799.

Higham, N. J. 1996. *Accuracy and Stability of Numerical Algorithms.* Society for Industrial and Applied Mathematics, Philadelphia.

Holman, M. J., and J. Wisdom 1993. Dynamical stability in the outer Solar System and the delivery of short period comets. *Astron. J.* **105**(5), 1987–1999.

Lecar, M., and F. A. Franklin 1973. On the original distribution of the asteroids, I. *Icarus* **20**, 422–436.

Levison, H. F., and M. J. Duncan 1994. The long-term dynamical behavior of short-period comets. *Icarus* **108**, 18–36.

Marsden, B. G. (Ed.) 1996. *Minor Planet Circulars*. Minor Planet Center, Cambridge, MA; also, Marsden, B. G. 1996. *Minor Planet Circulars*. http://cfa-www.harvard.edu/cfa/ps/mpc.html, 24 October 1996.

Newman, W. I., M. P. Haynes, and Y. Terzian 1989. Double galaxy redshifts and the statistics of small numbers. *Astrophys. J.* **344**, 111–114.

Newman, W. I., M. P. Haynes, and Y. Terzian 1992. Limitations to the method of power spectrum analysis: Nonstationarity, biased estimators, and weak convergence to normality. In *Statistical Challenges in Modern Astronomy* (E. D. Feigelson and G. J. Babu, Eds.), pp. 137–153, 161–162. Springer-Verlag, New York.

Newman, W. I., M. P. Haynes, and Y. Terzian 1994. Redshift data and statistical inference. *Astrophys. J.* **431**, 147–155.

Newman, W. I., F. Varadi, K. R. Grazier, and W. M. Kaula 1995. Mappings and integrators on the edge of chaos. *Bull. Am. Astron. Soc.* **27**, 1200.

Press, W. H., B. P. Flannery, S. A. Teukolsky, and W. T. Vetterling 1988. *Numerical Recipes in C: The Art of Scientific Computing*. Cambridge Univ. Press, New York.

Soper, P., F. Franklin, and M. Lecar 1990. Original distribution of the asteroids. II. Orbits between Jupiter and Saturn. *Icarus* **87**, 265–284.

Spitzer, L., Jr. 1962. *Physics of Fully Ionized Gases*, 2nd rev. ed. Interscience, New York.

Spitzer, L., Jr. 1987. *Dynamical Evolution of Globular Clusters*. Princeton Univ. Press, Princeton, NJ.

Stewart, G. R., and W. M. Kaula 1980. A gravitational kinetic theory for planetesimals. *Icarus* **44**, 154–171.

Stewart, G. R., and G. W. Wetherill 1988. Evolution of planetesimal velocities. *Icarus* **74**, 542–553.

Störmer, C. 1907. Sur les trajectories des corpuscles electrises. *Arch. Sci. Phys. Nat. Geneve* **24**, 5–18, 113–158, 221–247.

Sussman, G. J., and J. Wisdom 1988. Numerical evidence that the motion of Pluto is chaotic. *Science* **241**, 433–437.

Ward, W. R., and J. M. Hahn 1997. On stirring the Kuiper disk. *Bull. Am. Astron. Soc.* **29**, 1101.

Weibel, W. M., W. M. Kaula, and W. I. Newman 1990. A computer search for stable orbits between Jupiter and Saturn. *Icarus* **83**, 382–390.

Wisdom, J., and M. Holman 1991. Symplectic maps for the *N*-body problem. *Astron. J.* **102**, 1528–1538.